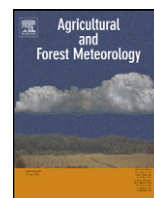




Contents lists available at ScienceDirect

## Agricultural and Forest Meteorology

journal homepage: [www.elsevier.com/locate/agrformet](http://www.elsevier.com/locate/agrformet)



# The challenges of measuring methane fluxes and concentrations over a peatland pasture

Dennis Baldocchi\*, Matteo Detto<sup>1</sup>, Oliver Sonnentag<sup>2</sup>, Joe Verfaillie, Yit Arn Teh, Whendee Silver, N. Maggi Kelly

Department of Environmental Science, Policy and Management, 130 Mulford Hall, University of California, Berkeley, Berkeley, CA 94720, USA

### ARTICLE INFO

#### Article history:

Received 6 December 2010  
Received in revised form 21 March 2011  
Accepted 15 April 2011

Dedicated to T. Andy Black.

#### Keywords:

Eddy covariance  
Peatland  
Wetland  
Cattle  
Rice  
Methane  
Laser spectrometer  
Biogeochemistry

### ABSTRACT

We report on methane (CH<sub>4</sub>) concentrations and efflux densities that were measured over a drained and grazed, peatland pasture in the Sacramento-San Joaquin River Delta of California over a three year period. The site was ideal for micrometeorological flux measurements due to its very flat topography, its exposure to vigorous winds and its extended fetch along the predominant wind direction. Nevertheless, the interpretation of methane fluxes with eddy covariance proved to be extremely complicated by a number of geographical, biophysical, biogeochemical and site management factors.

Initial inspection of the data revealed unexpected results—methane concentrations and efflux densities were greatest during the night rather than during the day. To explain this odd diurnal behavior in methane efflux densities and concentration, we tested two hypotheses. The prime hypothesis presupposed that the stable stratification of the nocturnal boundary layer elongated the flux footprint and enabled the flux tower to sense wetter fields at the western edge of the pasture, flooded drainage ditches, and/or a tidal marsh upwind of the pasture—these land forms emitted methane at rates 10–100 times greater than the drained portion of the peatland. And, this methane was emitted into a shallower volume of the atmosphere due to the collapse of the nocturnal boundary layer, causing methane concentrations to rise faster. The alternative hypothesis attributed the higher nocturnal methane fluxes to cattle, as they may have congregated near the tower at night.

We investigated these hypotheses with: (1) a series of micrometeorological field measurements at companion sites upwind and downwind of the pasture; (2) a series of chamber-based flux measurements on the representative land classes; (3) through the lens of a one-dimensional planetary boundary layer (pbl), box model; and (4) via inspection of digital camera images for the presence or absence of cattle. Together, these pieces of data suggest that elevated methane fluxes and concentrations at night were due to the combined correlation between: (1) the collapse of the nocturnal boundary layer; (2) the elongation of the flux and concentration footprints; and (3) the preferential sampling of an elevated methane source, be it the cattle, wet proportions of the field or some combination. On the other hand, our flux measurements were not perturbed by methane emanating from the tidal marsh that was several kilometers upwind of the peatland pasture site.

© 2011 Elsevier B.V. All rights reserved.

## 1. Introduction

The atmosphere's methane burden plays a major role in determining the atmosphere's climate and chemistry (Crutzen and Lelieveld, 2001; Khalil et al., 2007; Ramanathan et al., 1985); it is a greenhouse gas whose concentration has doubled since pre-

industrial times and whose warming potential is more than twenty times carbon dioxide.

Single-celled archaea are the dominant sources of methane. They inhabit anaerobic microsites in the soil and water-saturated zones laden with carbon (C), like freshwater marshes, peatlands, rice paddies and the stomachs of cows and termites. Archaea produce methane via two major routes (Conrad, 1996; Schimel, 2004; Whalen, 2005). One group of methanogens produces CH<sub>4</sub> by using hydrogen (H<sub>2</sub>) as an electron donor to reduce the CO<sub>2</sub> that evolves from fermented organic matter. Another major group of methanogens uses acetate (CH<sub>3</sub>COOH), formed from fermented organic matter, as a source of energy and splits it into CH<sub>4</sub> and CO<sub>2</sub>. Conversely, methane is consumed under aerobic conditions

\* Corresponding author. Tel.: +1 510 642 2874; fax: +1 510 643 5098.

E-mail addresses: Baldocchi@berkeley.edu (D. Baldocchi), DettoM@si.edu (M. Detto), oliver.sonnentag@gmail.com (O. Sonnentag).

<sup>1</sup> Present address: Smithsonian Institute, Panama.

<sup>2</sup> Present address: Harvard University, Cambridge, MA, USA.

by methanotrophic bacteria. Factors governing CH<sub>4</sub> production and consumption in freshwater marshes, peatlands and rice paddies include climate (temperature, light), biogeochemistry (plant productivity, carbon pool, soil oxygen concentration, and the presence or absence of alternative electron acceptors like iron, sulfate and nitrate), plant functional type (absence or presence of plants with conductive xylem, aerenchyma), soil physical properties (texture, porosity, bulk density, water filled pore space) and hydrology (soil moisture, water table depth, lateral flow rate) (Brinson et al., 1981; Holden, 2005; von Fischer and Hedin, 2007; Whalen, 2005; Whiting and Chanton, 1993). Methane transport between soil sediments and the atmosphere can be facilitated by ebullition (e.g. bubble transport) and xylem transport (Chanton et al., 1989; Holzapfel-Pschorn and Seiler, 1986). Conversely, methane transport can be hindered by slow diffusion across the water–air interface, through the tortuous soil column and via consumption by aerobic methanotrophs in aerated soil and water layers (Conrad, 1996), and by anaerobic methane oxidizers in anoxic conditions (Knittel and Boetius, 2009; Oremland and Culbertson, 1992).

The Sacramento–San Joaquin River Delta region is an ideal venue for studying CH<sub>4</sub> fluxes because it is replete in marshes and drained, agricultural peatlands. High CH<sub>4</sub> effluxes are expected from marshes in the Sacramento–San Joaquin River Delta because they overlay C-rich and anaerobic soils, the region experiences a long and warm growing season, and the ecosystem experiences high rates of net primary productivity (Brinson et al., 1981; Miller et al., 2001; Zhao et al., 2009). Drained peatlands create a complex landscape with methane-emitting hot and cold spots. This is because they overlay shallow water tables with methane-producing anaerobic zones, they are flooded periodically for irrigation, the fields are crossed with flooded drainage ditches (Teh et al., 2011) and many fields are grazed with cattle (Detto et al., 2010).

There are societal and policy-based reasons for studying methane exchange in the Delta, too. The Delta is a major conduit of water to the agricultural fields of the San Joaquin Valley and the burgeoning population of southern California. The future of Delta, however, is very uncertain and a subject to great debate. Current land management practices are not sustainable in the Delta as drainage over the last 130 years has caused more than 10 m of peat to be lost via subsidence, respiration and erosion (Drexler et al., 2009; Miller et al., 2008). Consequently, this landscape is vulnerable to sea level rise and flooding if the system of levees fail (Mount and Twiss, 2005; Syvitski et al., 2009). Efforts are underway to restore these drained peatlands to their native state with the reintroduction of wetland vegetation. While pilot studies show that ecological restoration is successful in sequestering carbon and building peat soils, it also produces methane at enhanced rates (Miller et al., 2008). Hence, baseline information on methane fluxes from drained peatlands is needed to advise how methane fluxes may change if peatland pastures and farmland are restored to native vegetation and wetlands.

We are entering a new era where quasi-continuous, eddy covariance measurement of methane exchange are possible over peatlands and wetlands (Detto et al., 2010; Hendriks et al., 2008; Rinne et al., 2007). This ability is associated with recent technological advances in commercially-available and affordable, tunable diode laser spectrometers that are suitable for measuring methane concentrations at sufficiently high sampling rates (Baer et al., 2002). In this light, we have been measuring methane concentration and flux densities with the eddy covariance technique over a peatland pasture in the Sacramento–San Joaquin River Delta of California, USA since April, 2007. The overarching objective of this paper is to report on the interpretation of temporal variability in CH<sub>4</sub> fluxes and concentrations measurements, across hourly, daily, seasonal, and annual time scales. Our ultimate goal is to produce data that

are relevant to the science, land management and policy issues we articulated above.

In conducting this study, we found that the interpretation of methane fluxes by eddy covariance measurements was much more complicated than measurements of carbon dioxide and water vapor fluxes (Baldocchi, 2003) even though this site was ideal from a micrometeorological perspective (Detto et al., 2010). This complication was produced by the presence of a heterogeneous field of methane sources upwind of the flux tower (Detto et al., 2010; Teh et al., 2011). To interpret the three-year time series at the peatland pasture site, we found it necessary to augment our eddy covariance flux measurements at the anchor site by: (1) conducting a series of flux density and concentration measurements at two companion sites—a rice paddy that was downwind and a tidal marsh that was upwind; (2) making a series of chamber-based flux measurements over the representative land forms; (3) interpreting our methane flux and concentration data through the lens of a one-dimensional planetary boundary layer (pbl), box model; and (4) inspecting a corresponding time series of digital images for the presence or absence of cattle.

## 2. Materials and methods

### 2.1. Site

The primary air sampling and flux measurement site was over a drained, peatland pasture on Sherman Island. This site is located on the west side of the Delta and at the confluence of the Sacramento and San Joaquin Rivers (lat: 38.0373N; long: 121.7536W; Elevation –12.1 m), near Antioch, CA (Fig. 1). The field sampling site was below sea-level (–10 m). The air sampling started in April, 2007, and continued until September, 2010. A second sampling site was established 11.6 km downwind on Twitchell Island in April, 2009 over a rice paddy (38°6.524'N; 121°39.181'W). We established a third sampling site during the spring of 2010 that was downwind from a tidal marsh (38°1.946'N; 121°46.332'W) and 1.62 km upwind of the peatland pasture.

The climate is Mediterranean, with wet cool winters and dry hot summers; mean annual rainfall is 325 mm and mean annual air temperature is 15.6 °C. And predominant winds come from the west. In general, we sampled air that passed over an extensive and very flat fetch (over 3000 m) of peatland pasture after it entered the Delta from the Pacific Ocean and crossed a large (~3–5 km) tidal marsh (Fig. 1), a potential source of methane (Hirota et al., 2007; Wang et al., 2009). The predominant flux footprints for daytime and nighttime conditions are shown in Fig. 2. The typical extent of daytime flux footprint was on the order of 250 m and confined to the well drained portions of the pad-dock. In comparison, the nighttime flux footprint extended about 750 m upwind of the tower and crossed drainage ditches and a wetter portion of the pasture (Detto et al., 2010). A set of corresponding flux measurements made with chambers found that the drained crowns within the daytime flux footprint emitted methane at a mean rate of  $0.96 \pm 0.19 \text{ nmol m}^{-2} \text{ s}^{-1}$  (Teh et al., 2011). The presence and absence of drainage ditches in our flux footprint is important because they are known to be hot-spots for methane production; the ditches emitted methane at a mean rate of  $449 \pm 75 \text{ nmol m}^{-2} \text{ s}^{-1}$  (Teh et al., 2011).

The pasture was vegetated with pepperweed (*Lepidium latifolium*), a perennial herb, and foxtail barley (*Hordeum murinum*), an annual grass; both are non-native, invasive species and common throughout the region. The soil was a silt loam, with 5–10% carbon, in the upper 60 cm. It overlaid a deep organic peat layer, which was over 20 m thick (Drexler et al., 2009). The water table ranged between 0.50 and 0.70 m below the soil surface and kept

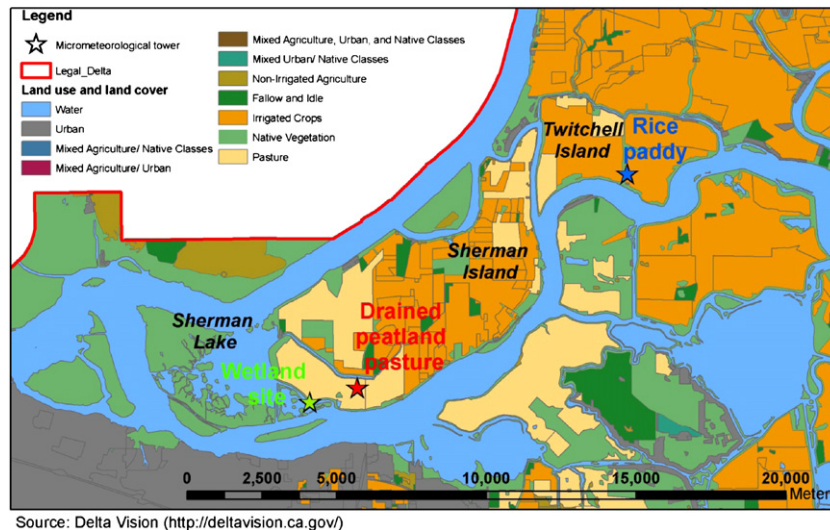


**Fig. 1.** Map of the sampling sites at the drained-peatland pasture on Sherman Island, the rice paddy on Twitchell Island and the marsh site upwind of the pasture. The stars denote the location of the flux towers.

the remnant peat in a saturated and anaerobic state, which favored methane production. The upper portion of vadose zone remained drained and aerobic by a system of drainage ditches.

2.2. Instrumentation

Methane concentrations were measured with a Los Gatos tunable diode laser spectrometer (DLT-100 Fast Methane Analyzer). Air was pulled through a 40 micron and two 2 micron filters with a dry scroll pump at a rate of 35 L min<sup>-1</sup> before entering the 0.408 L sampling cell. The instrument interrogated the air stream 10 times per second and 30 min averages were produced. Methane concentrations were sampled at a height of 3 m above the drained peatland pasture, and the rice paddy. And, we sampled air on the levee overlooking the tidal marsh at a height of 6.98 m with a second methane analyzer during the spring of 2010.

The CH<sub>4</sub> sensor used off-axis integrated cavity output spectroscopy (Baer et al., 2002; O’Keefe et al., 1999). A mid-infrared quantum cascade laser was tuned across the 6057 cm<sup>-1</sup> wavenum-

ber (1651 nm) CH<sub>4</sub> absorption band. The laser light was reflected between two curved mirrors multiple times to produce an optical path-length that was several km long. Light attenuation was measured directly and CH<sub>4</sub> concentrations were computed using Beer’s Law. To minimize pressure broadening, the cell pressure was maintained near 21.1 kPa with a mass flow controller. Because the laser was developed for commercial telecommunication purposes it did not require cooling by liquid nitrogen, making it conducive for continuous and unattended measurements. Together, these attributes produced an instrument that was based on fundamental physics, was highly accurate (±1%), precise (0.1%), experienced little drift (~10 ppb per week) and no interference by other trace greenhouse gases, like water vapor and CO<sub>2</sub>.

Field calibrations were performed on a regular interval (weekly to bi-weekly) using a primary standard gas that was traceable to the NOAA ESRL laboratory in Boulder Colorado; lab tests with a standard calibration gas produced concentration measurements with a precision of ±0.8 ppb out of a background of 1900 ppb when sampled at 1 Hz. The sensor signal, however, was noisier when sampled at 10 Hz (~±3 ppb). Consequently, the summation of instrument and geophysical noise was on the order of ±6 ppb when averaged over 30 min (Detto et al., 2010, 2011).

A suite of meteorological variables were measured in conjunction with the CH<sub>4</sub> concentrations. Wind and turbulence was measured with a three-dimensional sonic anemometer (Gill Windmaster Pro). Water vapor and carbon dioxide mole densities were measured with an open-path, infrared spectrometer (LICOR 7500, Lincoln, NE). Air temperature and humidity were measured with an aspirated and shielded thermistor and capacitance sensor (Vaisala HMP 45, Helsinki, Finland). Soil temperature was measured with a profile of copper-constantan thermocouples. Soil moisture was measured with a network of capacitance (ML2, Theta Probe, Delta-T Devices, Cambridge, UK) and time domain reflectometers (Moisture point PRB-K probes, Environmental Sensors Inc., Sydney, BC, Canada) sensors. Water table was measured with a pressure sensor (PDCR 1830-8388, Druck Pressure Transducer, Campbell Scientific, Logan, UT) immersed in a well, next to the meteorological tower.

The CH<sub>4</sub> sensor was integrated into an eddy covariance system to measure CH<sub>4</sub> fluxes (Detto et al., 2010, 2011). Methane efflux densities ( $F_{CH_4} = \bar{\rho}_a \overline{w' \chi'_{c, nat}}$ ) were computed in terms of the covariance between vertical wind velocity ( $w$ ) and mixing ratio ( $\chi_c$ ) fluctuations, times the density in dry air ( $\rho_a$ ). These covariances were corrected for density fluctuations due to water vapor ( $\chi_q$ )

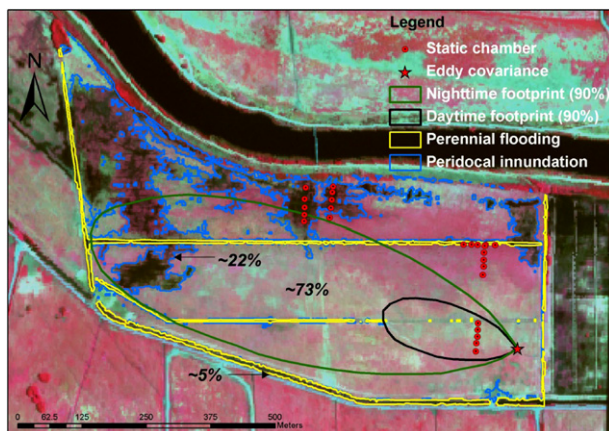


**Fig. 2.** Flux footprints along the predominant wind direction at the Sherman Island field site. The larger ellipse represents the nocturnal footprint and the smaller one is the daytime footprint. The nocturnal footprint overlays poorly drained areas of the pasture (noted by the dark spots, representing surface water) and drainage ditches, both of which represent methane hot spots. The footprint model was computed using the model of Detto et al. (2008). This figure was adapted from Detto et al. (2010) and Teh et al. (2010).

using the method of Detto and Katul (2007):

$$F_{\text{CH}_4} = \bar{\rho}_a \overline{w' \chi'_{c, \text{nat}}} = \bar{\rho}_a \left[ \overline{w' \chi'_{c, \text{nat}}} + \frac{\bar{\chi}_c}{\bar{\chi}_a} \overline{w' \chi'_{\text{q}}} \right] \quad (1)$$

We also corrected the covariances for time lags in the transport of air through the sampling tube and spectral attenuation of the sampling system. Details on computations are discussed in papers in other papers (Detto et al., 2010, 2011).

Because methane fluxes span such a wide range, it is important to assess the flux detection limit of our eddy covariance system. We estimated that the minimum detection limit of the eddy flux system was on the order of  $\pm 4 \text{ nmol m}^{-2} \text{ s}^{-1}$  (Detto et al., 2011). This detection limit was comparable to minimum  $\text{CH}_4$  fluxes reported in a number of methane flux studies that used the eddy covariance method (Hendriks et al., 2008; Rinne et al., 2007; Shurpali and Verma, 1998; Verma et al., 1992).

We subjected the methane flux time series to a number of quality assurance checks. First, we filtered and excluded data when the methane sensor or pump were not working, if the sampling rate had been reset at 1 Hz instead of 10 Hz after a power outage, if rain blocked the transmission of sound on the sonic anemometers or if the methane concentration was below ambient background conditions ( $< 1740 \text{ ppb}$ ). We also excluded data when friction velocity was below  $0.15 \text{ m s}^{-1}$  or exceeded  $1.2 \text{ m s}^{-1}$ , when methane effluxes were extreme ( $> 1500 \text{ nmol m}^{-2} \text{ s}^{-1}$ ) and when the standard deviation in methane concentration exceeded 35 ppb. Nevertheless, we did not find methane effluxes to be especially sensitive to friction velocity at night, as has been reported for  $\text{CO}_2$  exchange (Aubinet et al., 2000).

Background measurements of  $\text{CH}_4$  concentration were acquired from the NOAA ESRL laboratory field station at Trinidad Head ( $41.0537^\circ \text{N}$   $124.1534^\circ \text{W}$ ), in northern California (Dlugokencky et al., 2003). These  $\text{CH}_4$  concentrations are derived from weekly flask samples of air in the marine boundary layer.

To monitor field phenology and the presence or absence of cows, we installed a web camera (model DCS-900; D-Link Corporation, Taipei, Taiwan) and pointed it towards the west, the prevailing wind direction (Sonnentag et al., 2011). The presence or absence of cows within the vicinity of the meteorological tower was determined from the digital images through object-oriented image analysis. The index we developed was binary and detected if cows were present (1) or absent (0) in the image. The index did not reflect if the cows were close or far to the air sampling system. Additional information on the image analysis is provided in Appendix A.

### 3. Results and discussion

Over the course of this experiment we collected meteorological data for 61,392 thirty-minute intervals. Within this time frame, we collected 49,616 periods of data when the methane sensor was functioning and collected 32,212 periods of data when the wind direction was favorable and the sensors were functioning. To digest this large body of data, we first examine the seasonal variation in daily integrals of methane flux densities and concentrations. Then, we inspect the mean diurnal patterns of methane flux densities and concentrations for the dominant seasons. The intent is to describe their temporal behavior and identify the mechanisms that modulate the dynamics of methane concentrations and flux densities.

#### 3.1. Seasonal and diurnal variations in methane concentrations and fluxes

Over the multi-year sampling period—April 2007 through August 2010—daily-averaged, methane fluxes generally ranged between 0 and  $50 \text{ nmol m}^{-2} \text{ s}^{-1}$  during the dry

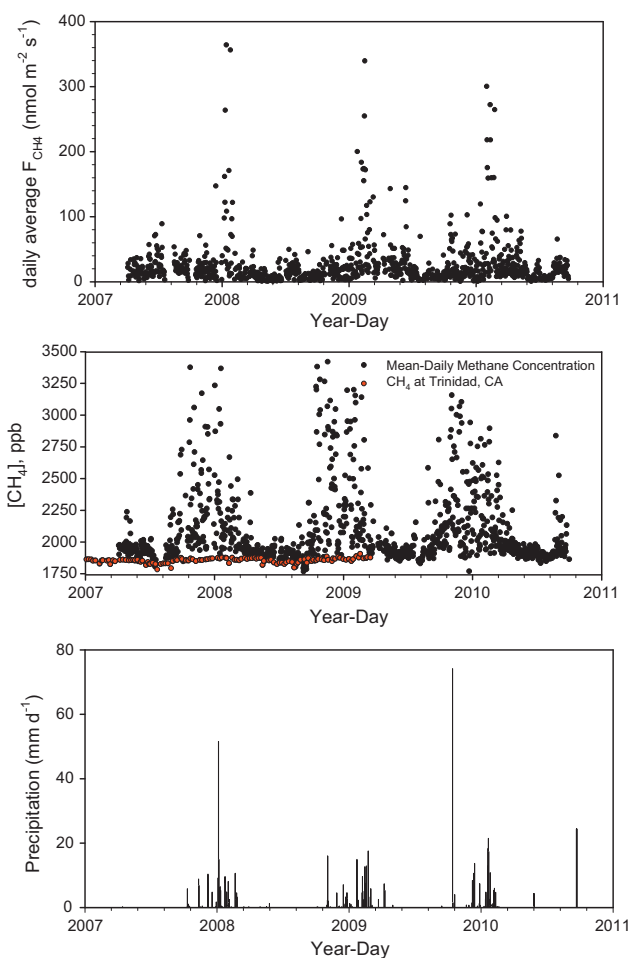


**Fig. 3.** Time series in: (a) daily-averaged methane flux densities; (b) daily-averaged  $\text{CH}_4$  concentration at Sherman Island, CA and weekly means from Trinidad, CA; (c) daily-integral of rainfall.

spring–summer–autumn period (days 100–300) (Fig. 3a). In contrast, we observed greater methane effluxes during the rainy autumn–winter–spring periods of the year (day  $< 100$  or day  $> 300$ ); then daily-averaged methane effluxes ranged between 50 and  $400 \text{ nmol m}^{-2} \text{ s}^{-1}$ .

Corresponding methane concentrations in the surface boundary layer exhibited considerable day-to-day variation in their daily-mean values (Fig. 3b). Mean-daily  $\text{CH}_4$  concentrations rarely exceeded 2000 ppb during the dry spring–summer–autumn period. In contrast, the majority of the highest  $\text{CH}_4$  concentrations ( $> 2000 \text{ ppb}$ ) occurred during the rainy season that extended between October and April.

Minimum methane concentrations were delineated by a boundary-line associated with the  $\text{CH}_4$  concentration of air entering the California coast, from the Pacific Ocean, as measured at Trinidad Head, CA (Fig. 3b). Minimum  $\text{CH}_4$  concentrations during dry summer days ( $\sim 1770 \text{ ppb}$ ) were about 100 ppb less than minimum concentrations during wet winter days ( $\sim 1870 \text{ ppb}$ ). The summertime minimum of the background  $\text{CH}_4$  concentrations suggests a net  $\text{CH}_4$  sink for air passing over the Pacific Ocean. This observation implies that the summertime increase in OH destruction of  $\text{CH}_4$  is greater than the seasonal and summertime increases in  $\text{CH}_4$  production from marshes and rice production (Dlugokencky et al., 1994; Steele et al., 1992).

Our minimum methane concentrations measurements were comparable with methane measured at 90 and 480 m on a tall television tower downwind from our field site at Walnut Grove,

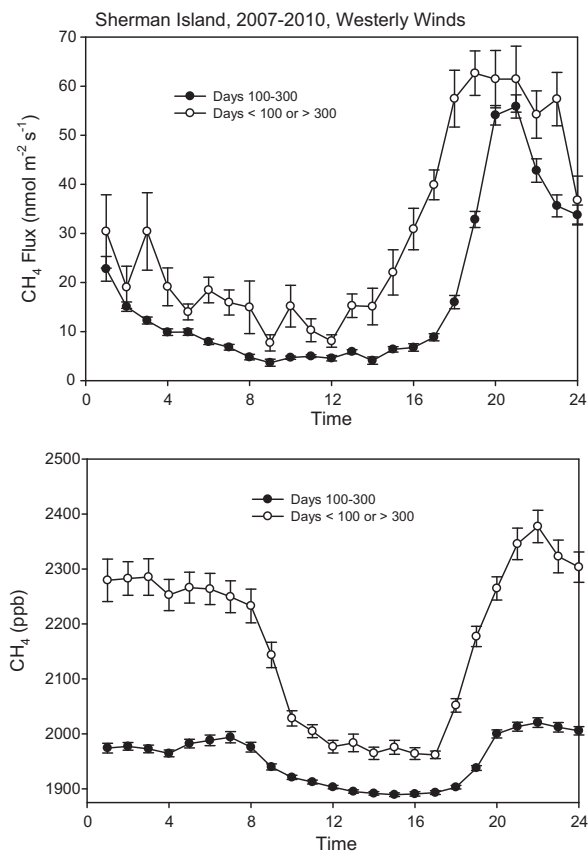


**Fig. 4.** Mean diurnal pattern of methane effluxes (a) and concentrations (b) for the dry spring–summer time period (days 100–300) and rainy period (days 300–100) for years 2007–2010. The data were filtered for conditions when winds came from the westerly sector ( $200\text{--}330^\circ$ ), retaining 52% of the data (32,212 thirty-minute sampling periods over a span of 61,392 periods). Standard errors are superimposed on the means.

CA (Zhao et al., 2009). The amplitude of the seasonal oscillation in daily minimum methane was similar to that observed in Hungary ( $\sim 100$  ppb) and greater than that typically observed across a global network of marine boundary layer sampling stations ( $\sim 30$  ppb) (Dlugokencky et al., 1994).

Fig. 4 distills other key information in Fig. 3 by reporting mean diurnal patterns in methane efflux densities (Fig. 4a) and concentrations (Fig. 4b) for the two distinct seasons, the dry period (days 100–300) and the rain period (days < 100 or days > 300), respectively. The mean diurnal behavior of methane effluxes and concentrations from the peatland pasture was unexpected. Lowest methane efflux densities occurred during the midday and the greatest efflux densities occurred after sunset and remained elevated throughout the night, during both the dry and wet periods. The lowest methane effluxes ( $0\text{--}10\text{ nmol m}^{-2}\text{ s}^{-1}$ ) were observed during the day and the dry period. These methane effluxes were representative of the well-drained portions of the field and were compatible with measurements from a companion spatial study made with chambers (Teh et al., 2011). Conversely, the higher methane efflux values ( $>50\text{ nmol m}^{-2}\text{ s}^{-1}$ ) that were observed at night during the dry period bisected the magnitude between methane rates lost from the drained and saturated portions of the field (Teh et al., 2011). Greatest methane efflux densities were observed during the rain period. For example, hourly-mean methane efflux densities ranged between 8 and  $63\text{ nmol m}^{-2}\text{ s}^{-1}$  during the wet period and hourly-mean methane effluxes ranged between 4 and  $56\text{ nmol m}^{-2}\text{ s}^{-1}$  during the dry period. This observation is con-

sistent with the expectation that wetter soils promote methane production and discourage methane consumption (Whalen, 2005).

At night, it was common to see mean CH<sub>4</sub> concentrations exceeding 2000 ppb during the dry period and reaching 2400 ppb during the wet period. In contrast, mean methane concentrations during the day were below 1900 ppb during the dry season and near 2000 ppb during the wet season.

These pronounced diurnal patterns, with strong nocturnal peaks in methane efflux densities and concentration, are the antithesis of typical diurnal patterns reported from Arctic and Boreal wetlands in Sweden, Finland, Canada and Minnesota (Jackowicz-Korczynski et al., 2010; Rinne et al., 2007; Shurpali and Verma, 1998), Californian rice paddies (McMillan et al., 2007) and Dutch peatlands (Hendriks et al., 2007, 2008); these comparative studies tend to report methane effluxes that peak during the day or are invariant over diurnal time scales. The data shown in Fig. 4 also differ greatly from the diurnal courses of methane fluxes made at this site with chambers—such effluxes were relatively invariant with time at a variety of land classes (Teh et al., 2011). The nocturnal peak in methane efflux densities is counter-intuitive if one expects a diurnal pattern to be modulated by temperature, which peaks during the day.

The highest nocturnal methane effluxes are especially notable, and merit additional scrutiny, because they exceed the geometric mean methane emission rates from an assortment of freshwater marshes (Bridgman et al., 2006) and ombrotrophic and minerotrophic peatlands in Scandinavia (Maljanen et al., 2010; Saarnio et al., 2007). These nocturnal peaks also merit more scrutiny because the areal extent of the hot-spot ditches is less than 10% of the area in the fetch.

### 3.2. Diagnosing why mean methane effluxes and concentrations peak at night

To explain why our diurnal time series in mean methane efflux and concentration is unique we propose and test two competing hypotheses. The first hypothesis involves the temporal modulation and covariation of the planetary boundary layer and the flux footprint. At night, the atmosphere becomes stably-stratified as the surface cools by radiating longwave energy (Mahrt, 1999). This phenomenon is accompanied with a collapse in the depth of the planetary boundary layer (Cleugh and Grimmond, 2001), a reduction in wind speed, and an extension of the flux and concentration footprints (Schmid, 2002; Vesala et al., 2008). If the elongated nocturnal flux footprint is seeing an elevated methane source area compared to the day, as suggested by Fig. 2, we hypothesize that larger methane effluxes and concentrations may result. This hypothesis is most plausible during the dry summer period when the western reach of the paddock and the drainage ditches that transect the pasture were often flooded (Fig. 2). Then these areas were landscape-scale, ‘hot-spots’ for CH<sub>4</sub> production; mean methane emissions rates from the drainage ditches ( $449 \pm 75\text{ nmol m}^{-2}\text{ s}^{-1}$ ) greatly exceeded those of all other landforms by up to 2 orders of magnitude (Teh et al., 2011). This hypothesis is least plausible during the winter when rain wets the entire field, in a more or less uniform manner.

The pasture was grazed year-round, too. So our alternative hypothesis invokes the role of cattle as significant methane sources (Laubach and Kelliher, 2005). If the cattle congregated within the near-field diffusion region of the measurement tower at night they could produce elevated methane effluxes and concentrations.

We test the plausibility of the former hypothesis by evaluating our methane fluxes and concentrations through the lens of a one-dimensional planetary boundary layer (pbl) box model. We tested the alternative hypothesis by measuring methane effluxes at auxiliary sites without cows. To accomplish this task, a set of methane

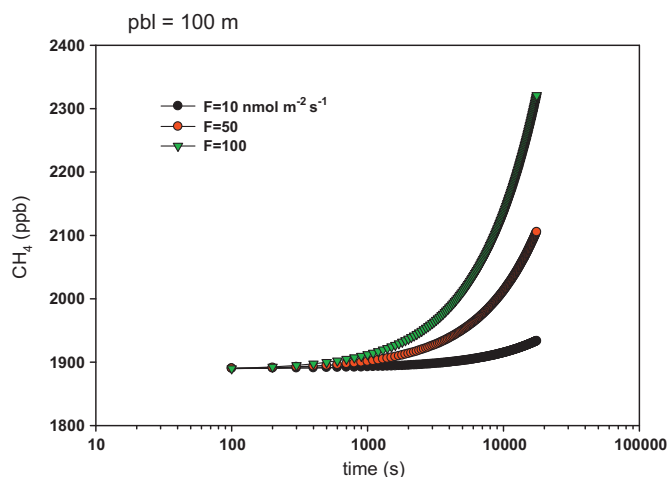


**Fig. 5.** Time series in computed methane concentration with the one-dimensional box model. This case is for a 100 m deep box and the methane concentration at time zero was 1890 ppb. Methane was emitted at rates of 10, 50 and 100  $\text{nmol m}^{-2} \text{s}^{-1}$ .

flux measurements were conducted over: (a) a flooded rice paddy, downwind from the pasture, and (b) a marshland, upwind of the pasture. We also inspected our web camera images for the presence or absence of cows when daytime methane efflux and concentration measurements were anomalous.

### 3.2.1. Nocturnal turbulence and the planetary boundary layer

The potential range of nocturnal  $\text{CH}_4$  concentrations and effluxes can be evaluated theoretically by considering a one-dimensional box model, which quantifies the time rate of change of  $\text{CH}_4$  ( $c$ ) as a function of the vertical flux divergence:

$$\rho_a \frac{\Delta c}{\Delta t} = -\frac{F_0}{z_i} \quad (2)$$

In the integral form, Eq. (2) can be expressed as:

$$c(t) = c(t_0) + \frac{F_0}{\rho_a z_i} (t - t_0) \quad (3)$$

In Eq. (2),  $\rho_a$  is the mole density of dry air,  $F_0$  is the  $\text{CH}_4$  efflux density at the surface and  $z_i$  is the depth of the inversion layer. In equation 3, the initial methane concentration ( $C(t_0)$ ) was 1890 ppb and the equation was integrated over a 10 h time span. We assumed that the top of the ‘box’ was delineated by the height of the nocturnal boundary layer ( $z_i$ ) and that the flux across this upper lid was nil. Consequently, the flux divergence is defined by the ratio of the surface flux density,  $F_0$ , and  $z_i$ .

Assuming that the nocturnal boundary layer collapses to a depth of 100 m in the Delta region (Cleugh and Grimmond, 2001; Zhao et al., 2009), we calculated that  $\text{CH}_4$  concentrations would not exceed 2000 ppb after 10,000 s (2.77 h) if the  $\text{CH}_4$  efflux of the daytime pasture footprint ( $\sim 10 \text{ nmol m}^{-2} \text{ s}^{-1}$ ) is representative of the landscape sensed by the  $\text{CH}_4$  sensor at night (Fig. 5). This set of computations is not supported by the observations shown in Fig. 4. On the other hand, our field observations are bounded by box model computations based on methane efflux rates of 50 and 100  $\text{nmol m}^{-2} \text{ s}^{-1}$ , as they produce  $\text{CH}_4$  concentrations that rise between 100 and 300 ppb above initial conditions, respectively, after 10,000 s.

Because our assumptions regarding depth of the nocturnal boundary layer and lack of entrainment are uncertain, we plotted  $\text{CH}_4$  concentrations as a function of  $\text{CH}_4$  efflux and planetary boundary layer depth to circumscribe the relationship between large  $\text{CH}_4$  concentrations, boundary layer depth and areally-integrated  $\text{CH}_4$  efflux. We found that  $\text{CH}_4$  concentrations exceeded 2300 ppb

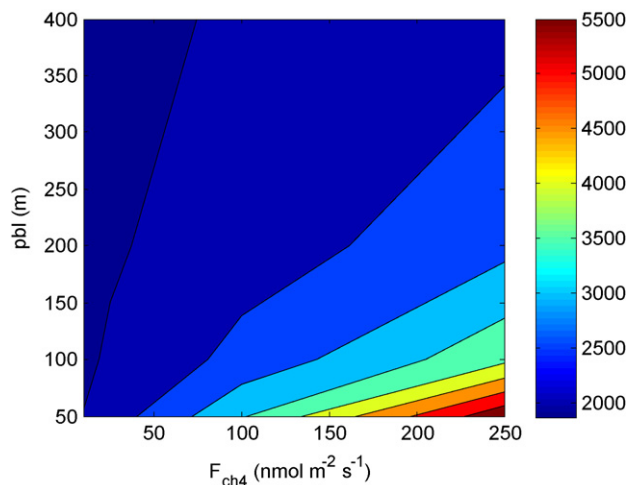


**Fig. 6.** Computation of  $\text{CH}_4$  concentrations using a one-dimensional box model for a stable and steady nocturnal boundary layer. The figure is plotted as a function of flux density ( $F_{\text{CH}_4}$ ,  $\text{nmol m}^{-2} \text{ s}^{-1}$ ) and height of the planetary boundary layer. The color contours represent methane concentration. These computations were derived after a time integral of 10 h.

(relative to the 1890 ppb initial condition) only during a distinct combination of conditions—when low boundary layer heights (50–350 m) corresponded with relatively high methane effluxes (50–250  $\text{nmol m}^{-2} \text{ s}^{-1}$ ) (Fig. 6).

These computations lead us to conclude that the large nocturnal methane concentrations may be explained by an elevated areal source emitting methane into a shallow boundary layer. At this stage, we cannot dismiss if the elevated methane source was associated with the elongation of the flux footprint over the wet areas of the paddock and the ditches as determined from our complimentary chamber studies (Teh et al., 2011). Nor, can we dismiss whether elevated methane effluxes (50–250  $\text{nmol m}^{-2} \text{ s}^{-1}$ ), that were inferred from the pbl model, were an artifact of the additive methane efflux from the herd of cattle.

### 3.2.2. Methane concentrations and flux densities at sites with extensive and homogeneous methane source fields, and without cows

Next, we examine mean diurnal patterns of methane effluxes and concentrations measured at the rice paddy down-wind from the pasture and the marsh upwind of the pasture to: (1) observe methane concentrations and fluxes at natural methane producing sites without cows; and (2) to examine if the mean diurnal patterns in methane flux densities and concentrations at these sites resemble those observed over the peatland pasture.

The mean diurnal pattern of methane efflux density over the downwind, rice paddy was relatively invariant over 24 h when the data were binned and averaged for periods corresponding with the dry period (days 100–300) or the rainy period (days < 100 or days > 300) (Fig. 7a). On the other hand, methane concentrations experienced much diurnal modulation, like those measured at the peatland pasture site (Fig. 7b).

The westerly fetch of the flux footprint at the rice paddy site was over 400 m so the sensor sampled air from the same methane producing source-field during the day and night, year-round; land further upwind of the rice was cultivated crops, which were not emitters of methane. Consequently, the temporal invariance in methane exchange over the rice provides a second piece of evidence suggesting that the elevated nocturnal methane fluxes observed over the peatland pasture may result from an elongation of the flux footprint, under a shallow and stable nocturnal boundary layer, that extends over upwind sources of methane. It is also noteworthy that

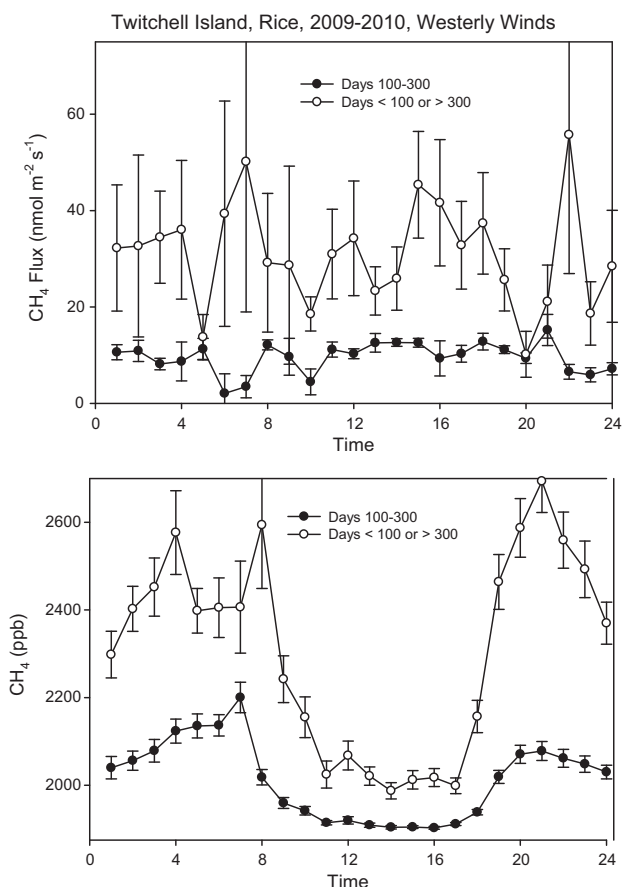


**Fig. 7.** Mean diurnal pattern of methane concentrations and effluxes over the rice paddy for the spring-summer time growing season period (days 100–300) and fallow, flooded autumn–winter period (days 300–100) for years 2009–2010. The data were filtered for conditions when winds came from the westerly sector (200–330°). Standard errors are superimposed on the means.

elevated methane concentrations were observed at night from the rice site, without cows. One plausible explanation for this observation is the fact that the rice field on Twitchell Island was downwind from a group of natural gas wells, which may leak some methane.

Next, we conducted a set of measurements upwind of the pasture, and downwind from a tidal marsh during the spring of 2010, until the solar panels were stolen by vandals. Data from the 26 day experiment showed moderate methane efflux densities (between 0 and 40 nmol m<sup>-2</sup> s<sup>-1</sup>, on average). The methane flux densities from the tidal marsh matched those emanating from the pasture during the day, but were exceeded by nocturnal effluxes from the pasture that, on average, approached 150 nmol m<sup>-2</sup> s<sup>-1</sup>. No distinct diurnal pattern in methane exchange (Fig. 8a) was observed from the tidal marsh, as compared to the corresponding set of measurements made at peatland pasture; methane concentrations downwind of the tidal marsh were generally below 1900 ppb and they tended to reach a maximum at mid morning rather than at night (Fig. 8b). This third piece of evidence allows us to accept the hypothesis that the anchor tower on the peatland pasture sensed elevated fluxes and concentrations at night because the elongation of the nocturnal flux footprint enabled the tower to sense elevated methane sources from the ditches and flooded portions of the field (Teh et al., 2011), or by cattle. It does not support the alternative hypothesis that tidal marsh, which was further upwind and produced smaller methane fluxes, contributed to the elevated nighttime fluxes and concentrations.

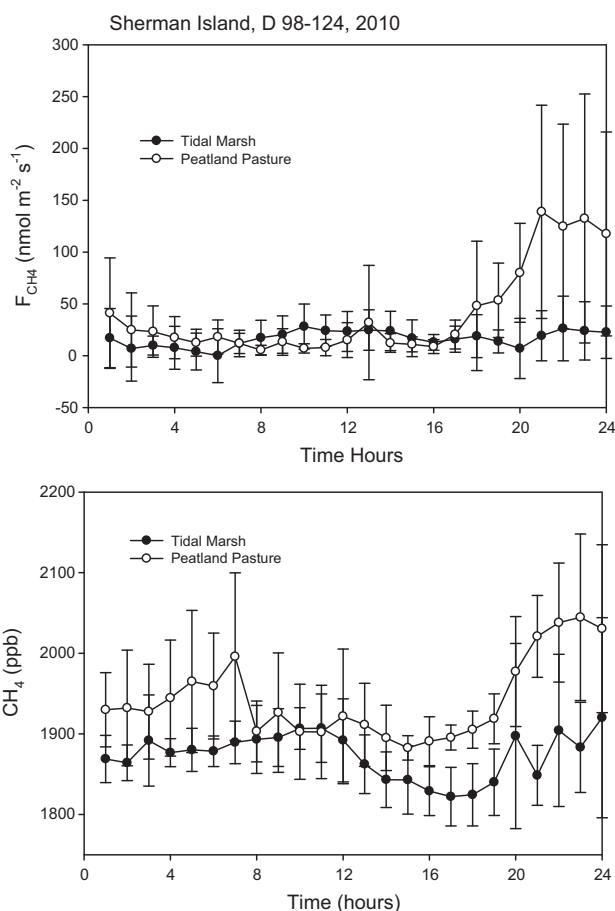


**Fig. 8.** Mean diurnal patterns in methane efflux and concentration from the tule marsh, upwind of the peatland, and the peatland pasture for the same period, days 98–124, 2010. Data were selected for periods with favorable wind direction.

### 3.2.3. Cattle, a mobile and intermittent methane source

During our frequent, daytime, site visits, we observed that the cattle often grazed near the far western side of the paddock and tended to be outside the flux footprint of the predominant winds. So we initially discounted their effect on our efflux and concentration measurements. Our thorough analysis of the data, however, forced us to re-consider the effects of grazing cattle on our methane concentration and flux measurements.

The paddock was about 0.38 km<sup>2</sup> in area and was grazed by about 100 cattle. If we assume that the cattle emitted between 10 and 20 mol of CH<sub>4</sub> per steer per day (Laubach et al., 2008; McGinn et al., 2009; van Haarlem et al., 2008), we compute a potential areal efflux density of CH<sub>4</sub> by the cattle to range between 30 and 60 nmol m<sup>-2</sup> s<sup>-1</sup>. These values suggest that the cattle had the potential to disturb our signal when they were close to the flux tower (e.g. within the near-field diffusion regime).

Using the object-oriented image processing methods to inspect the time series of digital images (Appendix A) we developed an index to deduce when cattle were present or absent in the images for the population of data. Fig. 9 shows that cattle were least prevalent during the afternoons of the dry period and most prevalent during the afternoons of the rainy period. There was also a tendency for cattle to congregate near the tower towards sunset of the dry period; the data suggest less so during the rain period. Unfortunately, the cow-cam was not capable of detecting the presence of cattle after sunset. But anomalous correlations between methane and carbon dioxide proved to be good indicators of the presence of cattle at night and were used to screen

**Table 1**  
Computation of annual methane effluxes with different assumptions on how the data are averaged and integrated.

	Variable footprint Day and night, with cows	Small footprint Day only, with cows	Large footprint Night only, with cows	Large–small footprint Night–Day, with cows	Small footprint Day only, without cows
$\text{gC m}^{-2} \text{y}^{-1}$	$8.66 \pm 6.65$	$4.2 \pm 1.93$	$13.1 \pm 6.67$	8.77	$2.68 \pm 1.42$
$\text{mol m}^{-2} \text{y}^{-1}$	$0.721 \pm 0.554$	$0.353 \pm 0.161$	$1.08 \pm 0.556$	0.73	$0.223 \pm 0.119$

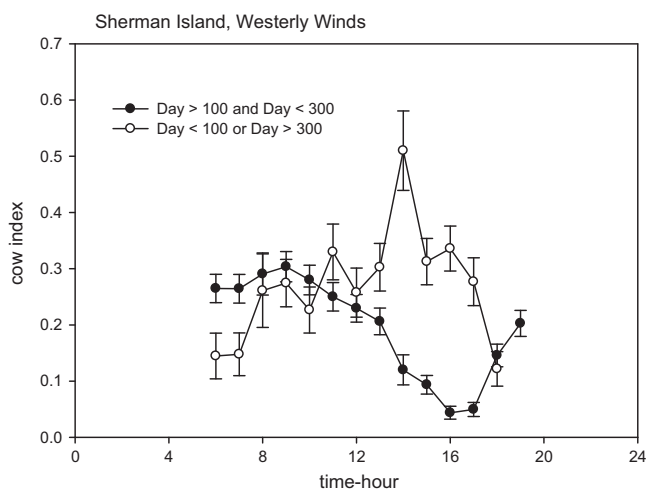


**Fig. 9.** The mean diurnal pattern of the fraction of cows in the region of interest in the digital camera image. Details on the cow index are reported in [Appendix A](#).

our data in other analyzes ([Detto et al., 2010, 2011](#); [Teh et al., 2011](#)).

With an ability to detect the presence and absence of cattle during the day, we filtered our data for periods when no cattle were present and winds were directed from the westerly fetch viewed by the camera. We then re-computed the mean diurnal pattern in methane flux density. [Fig. 10](#) shows slightly smaller methane efflux densities during the middle portion of day during the dry ( $4.2 \pm 1.88 \text{ nmol m}^{-2} \text{ s}^{-1}$ ) and wet ( $10.5 \pm 6.1 \text{ nmol m}^{-2} \text{ s}^{-1}$ ) periods. These values are significantly smaller than values reported in [Fig. 4](#) that contain elevated emissions from cows ( $5.77 \pm 1.59$  and  $17.8 \pm 9.35 \text{ nmol m}^{-2} \text{ s}^{-1}$ , for the dry and rainy periods, respectively).

[Fig. 10](#) also shows greatly elevated methane flux densities, in the absence of cows, as time approached sunset and the atmosphere became thermally stratified. Based on the set of experiments, model

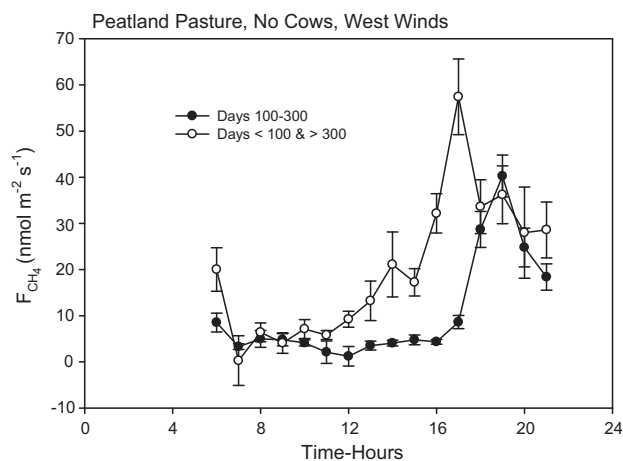


**Fig. 10.** Mean diurnal pattern in methane efflux when cows were absent in the image. The data were screened for the dry and periods and when winds came from the westerly sector that was viewed by the camera.

calculations and analysis of digital camera imagery, we cannot discount the combined effects of breathing cattle, the collapsed nocturnal boundary layer and the elongation of flux footprint over the methane hot spots in the field as co-varying factors contributing to elevated methane concentrations and efflux densities after sunset.

### 3.3. Constraining annual methane emission budgets

If we integrate the mean diurnal patterns and compute a mean annual methane efflux without any discrimination for cattle or elongated footprints we arrive at a value of  $0.721 \pm 0.554 \text{ mol m}^{-2} \text{ y}^{-1}$  or  $8.66 \pm 6.65 \text{ gC-CH}_4 \text{ m}^{-2} \text{ y}^{-1}$  ([Table 1](#)). For comparison, we estimated that the mean methane efflux from the landscape was  $9.5 \pm 3.4 \text{ gC-CH}_4 \text{ m}^{-2} \text{ y}^{-1}$  using a network of soil chambers ([Teh et al., 2011](#)); this estimate was derived from weekly chamber-based efflux measurements that sampled the representative land classes (crown, slope, hummock/hollow, drainage ditches) and was upscaled using remote sensing information that assessed their proportion of the total land area.

Rather than integrating all methane flux measurements, with all their attendant biases, the present study gave us guidance for producing conditional averages, which we use to bound the annual methane budget for the portion of the peatland sampled by the eddy covariance system. The mean daytime efflux of methane was  $11.2 \pm 5.1 \text{ nmol m}^{-2} \text{ s}^{-1}$ , after weighting the dry and rainy periods and favorable wind directions over three years ([Fig. 4](#)). If we accept that this value as representative of the 24 h average of methane that was emitted from the drained portion of the pasture, and that the emissions from the cows are minimal and diluted by the well mixed and deep daytime boundary layer, we compute an annual emission of  $0.353 \pm 0.161 \text{ mol m}^{-2} \text{ y}^{-1}$  or  $4.2 \pm 1.93 \text{ gC-CH}_4 \text{ m}^{-2} \text{ y}^{-1}$  ([Table 1](#)). In contrast, the mean nocturnal methane efflux was  $34.51 \pm 17.6 \text{ nmol m}^{-2} \text{ s}^{-1}$ , after weighting according to the wet and rainy periods. If we accept that this mean as representative of the methane emitted from the nocturnal flux footprint, which constitutes the aerated and wet portions of the field, and cows, we compute an annual emission of  $1.08 \pm 0.556 \text{ mol m}^{-2} \text{ y}^{-1}$  or  $13.1 \pm 6.67 \text{ gC-CH}_4 \text{ m}^{-2} \text{ y}^{-1}$ . And, we can estimate the methane emitted by the cattle and wetter patches by taking the differences between the day and night flux densities, with their different flux footprints, and sum that value over one year. This yields a mean difference of  $23.3 \text{ nmol m}^{-2} \text{ s}^{-1}$  and an annual sum of  $0.73 \text{ mol m}^{-2} \text{ y}^{-1}$  or  $8.77 \text{ gC-CH}_4 \text{ m}^{-2} \text{ y}^{-1}$  ([Table 1](#)).

If we use a smaller pool of data, sorted according to favorable wind directions and periods when no cows were detected in the camera image and assume these daytime conditions were representative of the whole day and year we calculate that the mean methane efflux density from the well-drained portion of the pasture was  $0.223 \pm 0.119 \text{ mol m}^{-2} \text{ y}^{-1}$  or  $2.68 \pm 1.42 \text{ gC-CH}_4 \text{ m}^{-2} \text{ y}^{-1}$ . Hence, we deduce that the drained portion of the peatland pasture was a very small source of methane. But we recognize that strong sources of methane exist in the region from cows, flooded areas of the field and drainage ditches. And that their presence can bias ones measurements and interpretation if ignored.

Year-long eddy covariance studies on methane emissions are relatively rare. For perspective, we cite three comparable cases. [Hendriks et al. \(2007\)](#) reported a loss of about  $30 \text{ g C-CH}_4 \text{ m}^{-2} \text{ y}^{-1}$

from a peatland in the Netherlands. Rinne et al. (2007) reported a loss of about  $9 \text{ g C-CH}_4 \text{ m}^{-2} \text{ y}^{-1}$  from a boreal fen in Finland. And Jackowicz-Korczynski et al. observed  $24 \text{ g C-CH}_4 \text{ m}^{-2} \text{ y}^{-1}$  were lost from an subArctic peatland. Our sums for the dry part of the peatland pasture are below these values and our sums for the wetter portion of the pasture resembles the boreal fen but remain lower than the amount of methane lost from the Dutch and the subarctic peatlands.

#### 4. Conclusion

Measuring greenhouse gas fluxes, which are produced solely by microbes, is much more complicated than measuring greenhouse gases that are routed through plants (e.g.  $\text{CO}_2$  and  $\text{H}_2\text{O}$ ), even over micrometeorologically ideal sites. Microbes produce hot and cold sources across a landscape that may vary by two to three orders of magnitude within a few meters, thereby challenging the assumption of a horizontally homogeneous source or sink (Baldocchi, 2003). This effect is not so evident over plant canopies, as they tend to fill space if there is adequate soil moisture and their spatial variability tends to be on the order of  $\pm 10\text{--}30\%$  (Hollinger et al., 2004).

The odd diurnal behavior in methane efflux and concentration observed over a peatland pasture forced us to conduct a series of micrometeorology field and modeling experiments that tested two plausible explanatory hypotheses. One explanatory hypothesis involved the collapse of the nocturnal boundary and the subsequent extension of the flux footprint under stable thermal stratification. The alternative explanation revolved around the hypothesis that cattle congregated around the tower at night and emitted methane at rates that outpaced efflux densities provided by the landscape—this herd was capable of emitting, on average, about  $100 \text{ nmol m}^{-2} \text{ s}^{-1}$  of methane.

The box budget computations, combined with digital camera images and field studies conducted upwind and downwind from the pasture, suggest that elevated methane fluxes and concentrations at night were due to the combined correlation between: (1) the collapse of the boundary layer; (2) the elongation of the flux and concentration footprints; and (3) the preferential sampling of an elevated methane source, be it the cattle, wet proportions of the field or some combination. We cannot disprove that cattle did not congregate near the flux tower after sunset on a semi-regular basis, but there was a tendency for them to approach the tower near sunset. On the other hand, our experiments indicate that we were not seeing elevated methane fluxes emanating from the tidal marsh that was several kilometers upwind of the peatland pasture site.

The findings reported here have important implications on the applicability and interpretation of eddy flux measurements to study methane and carbon dioxide exchange in intensively-managed peatland pastures. Cattle are typically present in peatland pastures, world-wide, and their presence complicates the interpretation of nocturnal methane effluxes. Extra pre-caution is needed to interpret methane fluxes and annual budgets at these sites. Consequently, the finding reported here may have implications on future interpretation of carbon dioxide emission records from intensively-grazed pastures (Gilmanov et al., 2007; Schulze et al., 2009; Soussana et al., 2007). We, thereby, recommend that practitioners conduct additional flux measurements at sites upwind and down wind and collect and inspect web camera imagery to decide when to accept and reject data.

The main drawback of our use of the web camera is that it only obtained data during the day. For future studies in pastures and rangelands where the presence of cattle might pose a challenge for the interpretation of eddy covariance measurements, we recommend the use of a 'game-cam'. This type of digital

camera was specifically designed for rugged outdoor applications in remote locations. Recently, game-cams have been used for phenological research given their repeat photography capabilities (Kurc and Benton, 2010). Game-cams are the simple digital cameras and their configuration requires only basic photographic understanding. Most game-cams allow for motion detection-triggered photography in addition to repeat photography, but the real advantage of some game-cams is the use an infrared flash to take black and white images at night. Considering that our object-oriented approach ignored spectral image attributes, we believe that future studies could employ our approach to detect cow absence and presence during the day and at night.

These  $\text{CH}_4$  concentration and flux measurements reported here have implications on land management. The first issue relates to the need to restore agricultural lands in the Delta to native vegetation, to stymie continued subsidence and safeguard the integrity of the levee system and protect the fresh water conveyance system upon which California relies (Mount and Twiss, 2005). Conversion of agricultural land back to native wetlands have the potential to produce larger  $\text{CH}_4$  sources (Miller et al., 2008), compared to the drained peatlands. Drained peatlands are shown to be small methane sources, but they are unsustainable in their present state as they are losing carbon. The second issue relates to the role of cows as strong methane emitters in grazed pastures. In this case the cows may be a larger source of methane than the land on which they graze. So it is incumbent upon researchers to evaluate their methane losses, too, if one is concerned about the methane burden upon the atmosphere. In our future work we intend to apply backward Lagrangian diffusion modeling (Flesch et al., 1995; Laubach et al., 2008; McGinn et al., 2009) to our extensive database and refine our estimate of the amount of methane emitted by the cattle. The third issue relates to global warming. These wetlands formed as the glaciers melted, sea level rose and vegetation was entombed in an anaerobic environment (Malamud-Roam et al., 2006). Further sea-level rise with the melting of the Greenland ice sheet and Antarctica will form more temperate wetlands, which may have a positive feedback on the climate system by emitting more  $\text{CH}_4$  into the atmosphere.

#### Acknowledgements

This work was funded by NSF-ATM grant number AGS-0628720 and the California Department of Water Resources grant #006550. We thank Mr. Ted Hehn for his able assistance in conducting the field measurements and servicing the instruments during the initial phase of the project. We thank Dr. Ed Dlugokencky and NOAA ESRL for the weekly of  $\text{CH}_4$  concentration from Trinidad Head, CA. We thank the California Department of Water Resources for permission to place our study site on their land and the land managers who maintained the rice study.

We thank Los Gatos Research for the loan of a mobile flux system for use during the spring of 2010.

#### Appendix A.

The diurnal and seasonal variation in the Cow Cam Index, detected with a digital camera. First, the JPEG files were converted to ENVI Image Files for analysis with the Feature Extraction Module in the ENVI/IDL image processing environment (ITT Visual Information Solutions). Next, we performed a principal component analysis on each image, and the first principle component was segmented into image objects within a defined region-of-interest. Then, the image objects were classified into "cow" and "non-cow" based on various spatial and texture attributes (Fig. A.1). Spectral attributes were ignored to minimize potential misclassification due to diurnal and seasonal effects of illumination changes (e.g., images taken

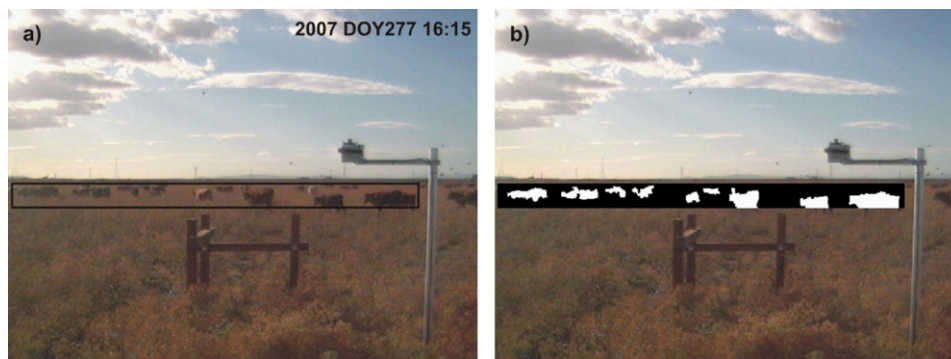


Fig. A.1. Digital camera image with cows (a) and with demarcation of the cows (b).

at dusk with the camera facing the Sun may result in very dark vegetation with spectral attributes similar to cows). For each resulting binary (cow vs. non-cow) region-of-interest we calculated a “cow-fraction” ( $f_{\text{cow}}$ ) with values from 0 to 1. Finally, the presence or absence of cows for a given region-of-interest was determined by median  $f_{\text{cow}}$  ( $f_{\text{cow-median}}$ ) for images with a  $f_{\text{cow}} > 0$ , with presence = 1 for  $f_{\text{cow}} > f_{\text{cow-aveage}}$  and absence = 0 for  $f_{\text{cow}} < f_{\text{cow-median}}$ . With this simple approach misclassifications were minimized and cows present at greater distance (>50 m) were ignored.

## References

- Aubinet, M., Grelle, A., Ibrom, A., Rannik, U., Moncrieff, J., Foken, T., Kowalski, A., Martin, P., Berbigier, P., Bernhofer, C., Clement, R., Elbers, J., Granier, A., Grunwald, T., Morgenstern, K., Pilegaard, K., Rebmann, C., Snijders, W., Valentini, R., Vesala, T., 2000. Estimates of the annual net carbon and water exchange of European forests: the EUROFLUX methodology. *Advances in Ecological Research* 30, 113–175.
- Baer, D.S., Paul, J.B., Gupta, J.B., O’Keefe, A., 2002. Sensitive absorption measurements in the near-infrared region using off-axis integrated-cavity-output spectroscopy. *Applied Physics B-Lasers and Optics* 75 (2–3), 261–265.
- Baldocchi, D.D., 2003. Assessing the eddy covariance technique for evaluating carbon dioxide exchange rates of ecosystems: past, present and future. *Global Change Biology* 9, 479–492.
- Bridgman, S.D., Megonigal, J.P., Keller, J.K., Bliss, N.B., Trettin, C., 2006. The carbon balance of North American wetlands. *Wetlands* 26 (4), 889–916.
- Brinson, M.M., Lugo, A.E., Brown, S., 1981. Primary productivity, decomposition and consumer activity in fresh-water wetlands. *Annual Review of Ecology and Systematics* 12, 123–161.
- Chanton, J.P., Martens, C.S., Kelley, C.A., 1989. Gas-transport from methane-saturated. Tidal fresh-water and wetland sediments. *Limnology and Oceanography* 34 (5), 807–819.
- Cleugh, H.A., Grimmond, C.S.B., 2001. Modelling regional scale surface energy exchanges and cbl growth in a heterogeneous, urban-rural landscape. *Boundary-Layer Meteorology* 98 (1), 1–31.
- Conrad, R., 1996. Soil microorganisms as controllers of atmospheric trace gases ( $\text{H}_2$ , CO,  $\text{CH}_4$ , OCS,  $\text{N}_2\text{O}$ , and NO). *Microbiological Reviews* 60 (4), 609–640.
- Crutzen, P., Lelieveld, J., 2001. Human impacts on atmospheric chemistry. *Annual Review of Earth and Planetary Sciences* 29 (1), 17–45.
- Detto, M., Katul, G., Mancini, M., Montaldo, N., Albertson, J.D., 2008. Surface heterogeneity and its signature in higher-order scalar similarity relationships. *Agricultural and Forest Meteorology* 148 (6–7), 902–916.
- Detto, M., Baldocchi, D., Katul, G.G., 2010. Scaling properties of biologically active scalar concentration fluctuations in the atmospheric surface layer over a managed peatland. *Boundary-Layer Meteorology* 136 (3), 407–430.
- Detto, M., Baldocchi, D., Anderson, F., Verfaillie, J., Xu, L., 2011. Comparing laser-based open- and closed-path gas analyzers to measure methane fluxes using the eddy covariance method. *Agricultural and Forest Meteorology*, submitted for publication.
- Detto, M., Katul, G.G., 2007. Simplified expressions for adjusting higher-order turbulent statistics obtained from open path gas analyzers. *Boundary-Layer Meteorology* 122 (1), 205–216.
- Dlugokencky, E.J., Houweling, S., Bruhwiler, L., Masarie, K.A., Lang, P.M., Miller, J.B., Tans, P.P., 2003. Atmospheric methane levels off: temporary pause or a new steady-state? *Geophysical Research Letters* 30 (19), 1992.
- Dlugokencky, E.J., Steele, L.P., Lang, P.M., Masarie, K.A., 1994. The growth-rate and distribution of atmospheric methane. *Journal of Geophysical Research-Atmospheres* 99 (D8), 17021–17043.
- Drexler, J.Z., de Fontaine, C.S., Deverel, S.J., 2009. The legacy of wetland drainage on the remaining peat in the Sacramento San Joaquin Delta, California, USA. *Wetlands* 29 (1), 372–386.
- Flesch, T.K., Wilson, J.D., Yee, E., 1995. Backward-time lagrangian stochastic dispersion models and their application to estimate gaseous emissions. *Journal of Applied Meteorology* 34 (6), 1320–1332.
- Gilmanov, T.G., Soussana, J.E., Aires, L., Allard, V., Ammann, C., Balzarolo, M., Barcza, Z., Bernhofer, C., Campbell, C.L., Cernusca, A., Cescatti, A., Clifton-Brown, J., Dirks, B.O.M., Dore, S., Eugster, W., Fuhrer, J., Gimeno, C., Gruenwald, T., Haszpra, L., Hensen, A., Ibrom, A., Jacobs, A.F.G., Jones, M.B., Lanigan, G., Laurila, T., Lohila, A., Manca, G., Marcolla, B., Nagy, Z., Pilegaard, K., Pinter, K., Pio, C., Raschi, A., Rogiers, N., Sanz, M.J., Stefani, P., Sutton, M., Tuba, Z., Valentini, R., Williams, M.L., Wohlfahrt, G., 2007. Partitioning European grassland net ecosystem  $\text{CO}_2$  exchange into gross primary productivity and ecosystem respiration using light response function analysis. *Agriculture Ecosystems & Environment* 121 (1–2), 93–120.
- Hendriks, D.M.D., Dolman, A.J., van der Molen, M.K., van Huissteden, J., 2008. A compact and stable eddy covariance set-up for methane measurements using off-axis integrated cavity output spectroscopy. *Atmospheric Chemistry and Physics* 8 (2), 431–443.
- Hendriks, D.M.D., van Huissteden, J., Dolman, A.J., van der Molen, M.K., 2007. The full greenhouse gas balance of an abandoned peat meadow. *Biogeosciences* 4, 411–424.
- Hirota, M., Senga, Y., Seike, Y., Nohara, S., Kunii, H., 2007. Fluxes of carbon dioxide, methane and nitrous oxide in two contrastive fringing zones of coastal lagoon, Lake Nakaumi, Japan. *Chemosphere* 68 (3), 597–603.
- Holden, J., 2005. Peatland hydrology and carbon release: why small-scale process matters. *Philosophical transactions of the royal society a-mathematical physical and engineering sciences* 363 (1837), 2891–2913.
- Hollinger, D.Y., Aber, J., Dail, B., Davidson, E.A., Goltz, S.M., Hughes, H., Leclerc, M.Y., Lee, J.T., Richardson, A.D., Rodrigues, C., Scott, N.A., Achuatavariar, D., Walsh, J., 2004. Spatial and temporal variability in forest-atmosphere  $\text{CO}_2$  exchange. *Global Change Biology* 10 (10), 1689–1706.
- Holzappel-Pschorn, A., Seiler, W., 1986. Methane emission during a cultivation period from an Italian rice paddy. *Journal of Geophysical Research-Atmospheres* 91 (D11), 1803–1814.
- Jackowicz-Korczynski, M., Christensen, T.R., Bäckstrand, K., Crill, P., Friberg, T., Mastepanov, M., Ström, L., 2010. Annual cycle of methane emission from a subarctic peatland. *Journal of Geophysical Research* 115 (G2), G02009.
- Khalil, M.A.K., Butenhoff, C.L., Rasmussen, R.A., 2007. Atmospheric methane: trends and cycles of sources and sinks. *Environmental Science & Technology* 41 (7), 2131–2137.
- Knittel, K., Boetius, A., 2009. Anaerobic oxidation of methane: progress with an unknown process. *Annual Review of Microbiology* 63, 311–334.
- Kurc, S.A., Benton, L.M., 2010. Digital image-derived greenness links deep soil moisture to carbon uptake in a creosotebush-dominated shrubland. *Journal of Arid Environments* 74 (5), 585–594.
- Laubach, J., Kelliher, F.M., 2005. Measuring methane emission rates of a dairy cow herd (II): results from a backward-Lagrangian stochastic model. *Agricultural and Forest Meteorology* 129 (3–4), 137–150.
- Laubach, J., Kelliher, F.M., Knight, T.W., Clark, H., Molano, G., Cavanagh, A., 2008. Methane emissions from beef cattle – a comparison of paddock-and animal-scale measurements. *Australian Journal of Experimental Agriculture* 48 (1–2), 132–137.
- Mahrt, L., 1999. Stratified atmospheric boundary layers. *Boundary Layer Meteorology* 90, 375–396.
- Malamud-Roam, F.P., Lynn Ingram, B., Hughes, M., Florsheim, J.L., 2006. Holocene paleoclimate records from a large California estuarine system and its watershed region: linking watershed climate and bay conditions. *Quaternary Science Reviews* 25 (13–14), 1570–1598.
- Maljanen, M., Sigurdsson, B.D., Guomundsson, J., Oskarsson, H., Huttunen, J.T., Martikainen, P.J., 2010. Greenhouse gas balances of managed peatlands in the Nordic countries – present knowledge and gaps. *Biogeosciences* 7 (9), 2711–2738.
- McGinn, S.M., Beauchemin, K.A., Flesch, T.K., Coates, T., 2009. Performance of a dispersion model to estimate methane loss from cattle in pens. *Journal of Environmental Quality* 38 (5), 1796–1802.

- McMillan, A.M.S., Goulden, M.L., Tyler, S.C., 2007. Stoichiometry of CH<sub>4</sub> and CO<sub>2</sub> flux in a California rice paddy. *Journal of Geophysical Research-Biogeosciences* 112 (G1), G01017.
- Miller, L.G., Kalin, R.M., McCauley, S.E., Hamilton, J.T.G., Harper, D.B., Millet, D.B., Oremland, R.S., Goldstein, A.H., 2001. Large carbon isotope fractionation associated with oxidation of methyl halides by methylotrophic bacteria. *Proceedings of the National Academy of Sciences of the United States of America* 98 (10), 5833–5837.
- Miller, R.L., Fram, M., Fujii, R., Wheeler, G., 2008. Subsidence reversal in a re-established wetland in the Sacramento-San Joaquin Delta, CA, USA. *San Francisco Estuary and Watershed Science* 6, 1–20.
- Mount, J., Twiss, R., 2005. Subsidence, sea level rise and seismicity in the Sacramento-San Joaquin Delta. *San Francisco Estuary and Watershed Science* 3, 18.
- O'Keefe, A., Scherer, J.J., Paul, J.B., 1999. CW integrated cavity output spectroscopy. *Chemical Physics Letters* 307, 343–349.
- Oremland, R.S., Culbertson, C.W., 1992. Importance of methane-oxidizing bacteria in the methane budget as revealed by the use of a specific inhibitor. *Nature* 356 (6368), 421–423.
- Ramanathan, V., Cicerone, R.J., Singh, H.B., Kiehl, J.T., 1985. Trace gas trends and their potential role in climate change. *Journal of Geophysical Research-Atmospheres* 90 (ND3), 5547–5566.
- Rinne, J., Riutta, T., Pihlatie, M., Aurela, M., Haapanala, S., Tuovinen, J.P., Tuittila, E.S., Vesala, T., 2007. Annual cycle of methane emission from a boreal fen measured by the eddy covariance technique. *Tellus Series B-Chemical and Physical Meteorology* 59 (3), 449–457.
- Saarnio, S., Morero, M., Shurpali, N.J., Tuittila, E., Mäkilä, M., Alm, J., 2007. Annual CO<sub>2</sub> and CH<sub>4</sub> fluxes of pristine boreal mires as a background for the lifecycle analysis of peat energy. *Boreal Environment Research* 7, 101–113.
- Schimel, J., 2004. Playing scales in the methane cycle: From microbial ecology to the globe. *Proceedings of the National Academy of Sciences of the United States of America* 101 (34), 12400–12401.
- Schmid, H.P., 2002. Footprint modeling for vegetation atmosphere exchange studies: a review and perspective. *Agricultural and Forest Meteorology* 113 (1–4), 159–183.
- Schulze, E.D., Luyssaert, S., Ciais, P., Freibauer, A., Janssens, I.A., Soussana, J.F., Smith, P., Grace, J., Levin, I., Thiruchittampalam, B., Heimann, M., Dolman, A.J., Valentini, R., Bousquet, P., Peylin, P., Peters, W., Rodenbeck, C., Etiope, G., Vuichard, N., Wattenbach, M., Nabuurs, G.J., Poussi, Z., Nieschulze, J., Gash, J.H., 2009. Importance of methane and nitrous oxide for Europe's terrestrial greenhouse-gas balance. *Nature Geoscience* 2 (12), 842–850.
- Shurpali, N., Verma, S., 1998. Micrometeorological measurements of methane flux in a Minnesota peatland during two growing seasons. *Biogeochemistry* 40, 1–15.
- Sonnentag, O., Detto, M., Vargas, R., Ryu, Y., Runkle, B.R.K., Kelly, M., Baldocchi, D.D., 2011. Tracking the structural and functional development of a perennial pepperweed (*Lepidium latifolium* L.) infestation using a multi-year archive of webcam imagery and eddy covariance measurements. *Agricultural and Forest Meteorology* 151, 916–926.
- Soussana, J.F., Allard, V., Pilegaard, K., Ambus, P., Amman, C., Campbell, C., Ceschia, E., Clifton-Brown, J., Czobel, S., Domingues, R., Flechard, C., Fuhrer, J., Hensen, A., Horvath, L., Jones, M., Kasper, G., Martin, C., Nagy, Z., Neftel, A., Raschi, A., Baronti, S., Rees, R.M., Skiba, U., Stefani, P., Manca, G., Sutton, M., Tubaf, Z., Valentini, R., 2007. Full accounting of the greenhouse gas (CO<sub>2</sub>, N<sub>2</sub>O, CH<sub>4</sub>) budget of nine European grassland sites. *Agriculture Ecosystems & Environment* 121 (1–2), 121–134.
- Steele, L.P., Dlugokencky, E.J., Lang, P.M., Tans, P.P., Martin, R.C., Masarie, K.A., 1992. Slowing down of the global accumulation of atmospheric methane during the 1980s. *Nature* 358 (6384), 313–316.
- Syvitski, J.P.M., Kettner, A.J., Overeem, I., Hutton, E.W.H., Hannon, M.T., Brakenridge, G.R., Day, J., Vorosmarty, C., Saito, Y., Giosan, L., Nicholls, R.J., 2009. Sinking deltas due to human activities 2 (10), 681–686.
- Teh, Y. et al., 2010. Large greenhouse gas emissions from agricultural and restored peatlands driven by management. *Ecosystems*, submitted for publication.
- Teh, Y., Silver, W., Sonnentag, O., Detto, M., Kelly, M., Baldocchi, D., 2011. Large greenhouse gas emissions from a temperate peatland pasture. *Ecosystems* 14, 311–325.
- van Haarlem, R.P., Desjardins, R.L., Gao, Z., Flesch, T.K., Li, X., 2008. Methane and ammonia emissions from a beef feedlot in western Canada for a twelve-day period in the fall. *Canadian Journal of Animal Science* 88 (4), 641–649.
- Verma, S.B., Ullman, F.G., Billesbach, D., Clement, R.J., Kim, J., Verry, E.S., 1992. Eddy-correlation measurements of methane flux in a northern peatland ecosystem. *Boundary-Layer Meteorology* 58 (3), 289–304.
- Vesala, T., Kljun, N., Rannik, U., Rinne, J., Sogachev, A., Markkanen, T., Sabelfeld, K., Foken, T., Leclerc, M.Y., 2008. Flux and concentration footprint modelling: state of the art. *Environmental Pollution* 152 (3), 653–666.
- von Fischer, J.C., Hedin, L.O., 2007. Controls on soil methane fluxes: tests of biophysical mechanisms using stable isotope tracers. *Global Biogeochemical Cycles* 21, GB2007.
- Wang, D., Chen, Z., Xu, S., 2009. Methane emission from Yangtze estuarine wetland, China. *Journal of Geophysical Research* 114 (G2), G02011.
- Whalen, S.C., 2005. Biogeochemistry of methane exchange between natural wetlands and the atmosphere. *Environmental Engineering Science* 22 (1), 73–94.
- Whiting, G.J., Chanton, J.P., 1993. Primary production control of methane emission from wetlands. *Nature* 364, 793–794.
- Zhao, C.F., Andrews, A.E., Bianco, L., Eluszkiewicz, J., Hirsch, A., MacDonald, C., Nehrkorn, T., Fischer, M.L., 2009. Atmospheric Inverse Estimates of Methane Emissions from Central California. *Journal of Geophysical Research, Atmospheres* 114, doi:10.1029/2008JD011671.